DE GRUYTER e-Polymers 2017; 17(4): 275–282

Kai Liang*, Gen Li, Meixuan Peng and Qingquan Liu*

Macroporous polymer beads derived from a novel coporogen of polyethylene/dichlorobenzene

DOI 10.1515/epoly-2016-0301
Received November 13, 2016; accepted January 23, 2017; previously published online March 28, 2017

Abstract: Macroporous poly(divinylbenzene) (PDVB) beads were prepared by traditional suspension polymerization in the presence of dichlorobenzene (DCB) and polyethylene (PE) as coporogen. Two types of PE with different molecular weights were used as polymer porogen, and the weight percent of PE in DCB varied from 0 to 8.0 wt%. Effects of PE concentration and PE molecular weight on the pore structure of PDVB beads were investigated. As expected, the highest surface area was achieved by the beads prepared with DCB as the sole porogen. Applying coporogen with PE with low molecular weight (LPE) content, the surface area of PDVB beads declined because of early phase separation induced by the cooperation of LPE and DCB. However, the value increased abruptly when 5 wt% LPE in DCB was used as coporogen. Subsequently, the values again decreased when LPE amount further increased. Overall, the molecular weight of PE and the concentration of PE in coporogen had a significant effect on the pore structure and surface morphology of PDVB beads.

Keywords: adsorption; coporogen; electron microscopy; polymers; porous materials.

1 Introduction

Macroporous polymer beads can find potential applications in the fields such as ion-exchange resins, adsorbents, column-packing materials for HPLC, catalyst support, and nanoparticle growth templates (1–3). In different application fields, different pore structures are required for macroporous polymer beads. Consequently, for many years the preparation of macroporous polymer beads with controllable pore structure was an important issue and received many attention (4, 5).

To date, linear polymers in combination with various organic solvents were widely used for the preparation of porous polymer beads such as the multistep seeded polymerization of Bradford and Vanderhoff (6), the activated swelling and polymerization techniques of Ugelstad et al. (7), and the dynamic swelling method proposed by Okubo and Nakagawa (8). Cheng et al. (9, 10) prepared macroporous polymer beads with polystyrene/toluene and polystyrene/hexane as coporogens and found that as the molecular weight of polystyrene increased, the peaks of the pore size distribution curves moved toward larger pores. Frechet et al. (11, 12) obtained similar results via generating macroporous polymer beads with polystyrene/dibutyl phthalate and styrene-methyl methacrylate copolymers/dibutyl phthalate as coporogens. Generally, the route of seed swelling polymerization can increase the pore diameter of polymer beads; however, the surface area derived from this route is relatively low (<100 m^2/g) (13, 14). The problem can be solved by suspension polymerization. For example, Macintyre and Sherrington (15) produced macroporous beads with poly(propylene glycol)/toluene and polydimethylsiloxane/toluene as coporogens via suspension polymerization and found that the surface area of the products could achieve 800 m^2/g. However, it is still a difficult issue to prepare macroporous polymer beads with fine tunable pore structure. Therefore, it will be valuable to explore novel coporogens to prepare macroporous beads with controllable pore structure.

Our previous works (16) indicated that poly(divinylbenzene) (PDVB) beads with high surface area could be achieved using dichlorobenzene (DCB) as the sole porogen. In another work, poly(propylene) in combination with toluene was used as coporogen to prepare PDVB beads with tunable porosity (17). Recently, our group (18) prepared monodisperse cross-linked polymer nanospheres via emulsifier-free miniemulsion polymerization and post cross-linking route without any porogens. However, the specific surface area of the nanoshperes was less than 100 m^2/g. In order to further investigate the effect of different linear polymer porogen on pore structure of PDVB beads, here, we attempt to prepare macroporous PDVB beads using polyethylene

---

***Corresponding authors: Kai Liang,** Department of Environmental Engineering, Shaoguan College, Shaoguan 512000, China, e-mail: liangkai2013@hotmail.com; and **Qingquan Liu,** Institute of Materials Science and Engineering, Hunan University of Science and Technology, Xiangtan 411201, China, e-mail: qqliu@hnust.edu.cn
Gen Li and Meixuan Peng: Institute of Materials Science and Engineering, Hunan University of Science and Technology, Xiangtan 411201, China

(PE) with different molecular weights and DCB as coporogen. Effects of PE concentration in coporogen and the molecular weight of PE on porosity of macroporous PDVB beads were studied.

2 Experimental

2.1 Materials

Divinylbenzene (DVB) was purchased from Sigma-Aldrich Chemie, Shanghai, China and used after purification. DVB was first extracted with 5 wt% NaOH solution to remove inhibitor, and then was washed with deionized water until neutralization. Second, DVB was dried by anhydrous magnesium sulfate. Finally, DVB was separated by vacuum distillation. PE with low molecular weight (LPE) and PE with high molecular weight (HPE) were prepared in our lab according to the Xiao et al. (19). 2,2′-Azo-bis-isobutyronitrile (AIBN) was provided by Linfeng Chem Co. Ltd., Shanghai, China. AIBN was used as the initiator after recrystallized from methanol. Poly(vinyl alcohol) (PVA, 88% hydrolyzed) and DCB were bought from the Aldrich Chemical Co., Shanghai, China and used without further purification.

2.2 Suspension polymerization

One hundred and twenty cubic centimeter of aqueous solution containing 1.0 g PVA and 3.96 g NaCl was charged into a three-neck glass reactor. The solution was stirred at a speed of 300 rpm and kept at 80°C. Porogen or coporogen with AIBN and DVB was added into the reactor. The polymerization was performed at 80°C for 6 h. The final products were first washed twice with hot water and then three times with methanol. PDVB beads were extracted with toluene for 24 h in a Soxhlet to remove PVA, PE porogen, and residual monomers. Finally, macroporous PDVB beads were dried in a vacuum oven at 50°C for at least 12 h.

2.3 Characterization

Micromeritics ASIC-2 instrument (Micromeritics, USA) was used for porosity analysis of macroporous PDVB beads. PDVB beads were first degassed at 70°C for 12 h to remove adsorbed materials, and then porosity analysis of PDVB beads was conducted at the temperature of liquid nitrogen (77.3 K). The surface area, the average pore diameter, and the pore size distribution curve were calculated using the standard software. In addition, the pore area, the average pore size, and the porosity of PDVB beads were also measured by an Autopore IV 9500 instrument. Surface morphologies of PDVB beads were determined by a scanning electron microscope (SEM, HITACHI, S4800, Japan).

3 Results and discussion

3.1 Preparation of macroporous PDVB beads

To investigate the effects of linear polymer porogen, and its molecular weight on the pore structure of macroporous PDVB beads, two types of PE (LPE: $M_n = 534$, PDI = 1.85; HPE: $M_n = 3.5 \times 10^4$, PDI = 2.41) prepared in-house (19) in combination with DCB were used as coporogen to prepare macroporous PDVB beads. Note that the concentration of LPE or HPE in DCB was no more than 8.0 wt% because of the difficult operation derived from the very high viscosity of coporogen. The details about the weight percent of LPE or HPE in DCB are presented in Table 1.

3.2 SEM images of macroporous PDVB beads

The surface morphologies of PDVB beads were observed by SEM, and some representative images (E20, E26, E28, E31, E36, and E38) are presented in Figure 1.

We could hardly find some differences in the low magnification images of PDVB beads prepared with LPE/DCB or HPE/DCB as coporogen. However, high magnification

Table 1: LPE and HPE concentration in DCB.

Run	E20	E22	E23	E24	E25	E26	E28
Weight percent of LPE in coporogen (wt%)	0	2	3	4	5	6	8
Run	E20	E31	E32	E33	E36	E38	–
Weight percent of LPE in coporogen (wt%)	0	1	2	3	6	8	–

AIBN, 0.033 g; DVB, 3.0 ml; coporogen of LPE/DCB or HPE/DCB, 3.0 ml.
Reaction time and temperature, 6 h/80°C.

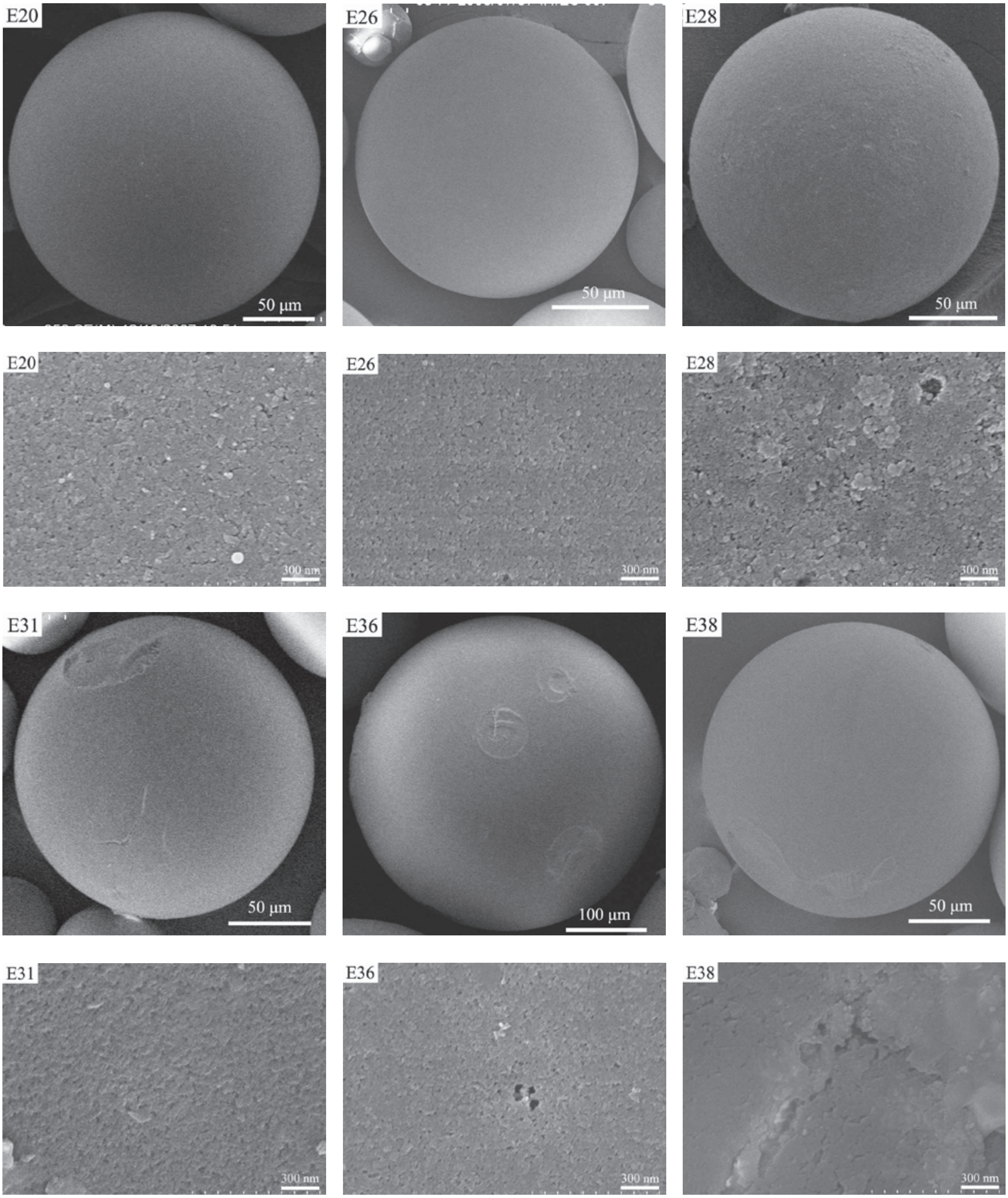

Figure 1: SEM images of macroporous PDVB beads prepared with LPE/DCB (E20, E26, and E28) and HPE/DCB (E31, E36, and E38) as coporogen.

images still revealed some discrepancies. For example, E20 displayed a rather uniform surface texture and some macropores, whereas E28 and E36 exhibited more macropores than that of E20. Furthermore, there were some ditch-shaped cracks on the surface of E38. These facts indicated that LPE or HPE porogen had an effect on the surface morphologies of macroporous PDVB beads. We speculated that higher molecular weight of polyethylene could result in an early phase separation, which was responsible for the different pore morphologies.

Table 2: Characterization data of macroporous PDVB derived from N_2 sorption and Hg intrusion.

Run	C-Pg[a] (wt%)	SSA[b] (m^2/g)	PA[c] (m^2/g)	APD[d]/nm		TPV[e]/cm^2/g		Hg porosity/%	
				N_2	Hg	N_2	Hg	3–50 nm	50–4000 nm
PDVB beads prepared using LPE/DCB as coporogen									
E20	0	813	138	3.9	14.9	0.79	0.51	15.7	4.3
E22	2	757	99	3.2	28.4	0.60	0.70	13.6	9.3
E23	3	728	80	3.2	27.8	0.58	0.56	14.3	6.8
E24	4	739	79	3.1	32.8	0.58	0.65	13.9	8.6
E25	5	807	167	4.4	15.2	0.89	0.64	17.1	6.1
E26	6	733	103	3.2	25.3	0.58	0.66	16.1	8.7
E28	8	706	126	3.5	23.9	0.62	0.75	14.5	9.5
PDVB beads prepared using HPE/DCB as coporogen									
E20	0	813	138	3.9	14.9	0.79	0.51	15.7	4.3
E31	1	798	177	4.2	15.7	0.84	0.69	16.1	6.2
E32	2	783	161	4.3	15.9	0.84	0.64	16.8	6.1
E33	3	784	163	3.7	14.2	0.73	0.58	15.9	5.5
E36	6	722	100	3.2	22.1	0.54	0.56	14.3	6.2
E38	8	685	95	3.2	33.0	0.57	0.78	13.3	11.6

[a] C-Pg, the weight percent of LPE or HPE in DCB.

[b] SSA, the specific surface area got from N_2 sorption.

[c] PA, the pore surface derived from Hg intrusion.

[d] APD, the average pore diameter originated from N_2 sorption and Hg intrusion.

[e] TPV, the total pore volume originated from N_2 sorption and Hg intrusion.

3.3 Effects of LPE and HPE porogen on the pore structure of PDVB beads

Porosity of PDVB beads was characterized by N_2 sorption and Hg intrusion, and the results are summarized and presented in Table 2.

3.3.1 Effects of LPE and HPE on the surface area

With LPE concentration increasing, the surface area of PDVB beads (E20–E28) underwent a trend of decline, increase, and decline again. The maximum value (813 m^2/g) was achieved by E20, which was prepared with DCB as the sole porogen (16). The fact that DCB is the thermodynamically compatible solvent of polystyrene should be responsible for the maximum value because compatible solvent will induce a late phase separation of PDVB. The first decline of the surface area was due to low-level HPE (2.0–3.0 wt%), and DCB induced an earlier phase separation in comparison with E20. However, as LPE content further increased (4.0–5.0 wt%), the surface area of E24 and E25 exhibited an increase instead of a fall. Interestingly, after the weight percent of LPE exceeded 6.0 wt% (E26 and E28), the surface area decreased again. These facts could be explained and understood by the theory of double-phase separation.

Double separation was invoked by Macintyre and Sherrington (15), who prepared PDVB beads with poly(propylene glycol) or poly(dimethylsiloxane) oligomers and toluene as coporogen. The author suggested that because of different compatibilities with PDVB network, oligomer induced the earlier phase separation, and toluene resulted in the later one. However, we speculated that double separation only occurs when the content of polymer porogen exceeds a certain value, which strongly depends on the molecular weight of linear polymer.

When LPE content was 2, 3, and 4 wt%, there may be two cases about phase separation. First, low level of incompatible LPE had a little effect on PDVB network; as a consequence, the cooperation of LPE and DCB might give rise to a single earlier phase separation in relative to the sole porogen of DCB. Second, there might be double-phase separation, but they overlapped because of low-level LPE. In this case, it was not a real double-phase separation but a prolonged one. Therefore, it is suggested that coporogen with low-level LPE just lead to larger gel particles in contrast to the sole porogen of DCB. The facts reduced the surface area of E22, E23, and E24.

After LPE content achieved 5 wt% (E25), the amount of LPE was high enough to induce a dependent double-phase separation. The macroporous networks induced by LPE porogen improved pore connection of PDVB beads (17), which increased the surface area of E25. It should

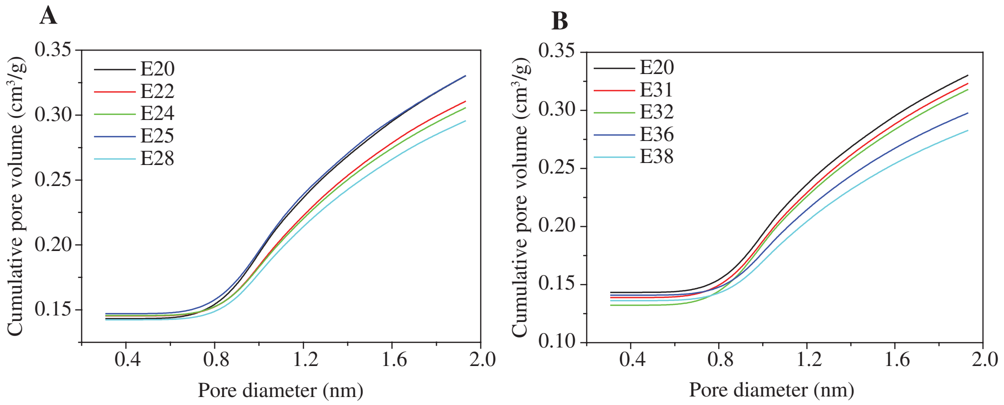

Figure 2: Cumulative pore volume calculated by the Horvath-Kawazoe method (carbon-slit pore model) in the range of micropores (< 2 nm).

be noticed that the surface area of E25 was still less than that of E20. However, our previous work indicated that the maximum of surface area was achieved with 2 wt% poly(propylene)/toluene coporogen instead of the sole porogen of toluene (17). A similar result was also obtained by Macintyre and Sherrington (15). In fact, DCB is a better porogen than toluene in the generation of PDVB beads with high porosity.

With further increasing LPE level (E26 and E28), because of much earlier phase separation induced by LPE, larger gel particles were generated during the first phase separation. Although the second phase separation still formed some small gel particles, the surface area of E26 and E28 still decreased because of larger gel particles formed in the first phase separation. Anyway, the surface area of as-prepared PDVB beads was higher than that derived from seed swelling polymerization (9–13).

The surface area trend of PDVB beads produced from HPE/DCB coporogen was different with that from LPE/DCB coporogen. With increasing HPE level, the surface area of PDVB beads declined progressively. We think the high molecular weight of HPE should be responsible for that. The incompatibility between PE and PDVB network was greatly enhanced as the molecular weight of PE increased sharply. Although the content of HPE was just 1 wt%, it was high enough to induce a dependent double-phase separation. As HPE level further increased (E32–E38), much earlier phase separation resulted in larger gel particles, which decreased the surface area of PDVB beads.

3.3.2 Effects of LPE or HPE on the pore area

The pore area derived from Hg intrusion could reflect pore connectivity of macroporous PDVB beads, which could be improved by the larger gel particles induced by the first phase separation (15). As shown in Table 2, the variation trend of pore area was similar to that of surface area. The pore area was declined from E20 to E24 until the weight percent of LPE amounted to 5 wt%. The value of E25 increased abruptly to 167 m^2/g, which was even higher than that of E20. This fact revealed that E25 had excellent pore connectivity, which was originated from the first phase separation induced by LPE. As the concentration of HPE was further increased, the values of E26 and E28 were decreased again. However, it should be noted that the pore areas of E26 and E28 were still higher than those of E22, E23, and E24. This result was agreement with that discussed above, namely, a prolonged single-phase separation of E22, E23, and E24 failed to improve the pore connectivity.

As for PDVB beads derived from HPE/DCB coporogen, the maximum pore area was achieved by E31. This is easy to understand. Low HPE level in coporogen could also give rise to a dependent phase separation. Moreover, the values of E31, E32, and E33 were even higher than that of E20. It should be noted that a combination between high surface area and excellent pore connectivity could be achieved by tuning LPE or HPE amount in coporogen. We believe this result will be valuable for improving properties of the absorbents with high surface area and pore connectivity.

3.3.3 Effects of LPE or HPE on porosity

The pore volume from N_2 sorption and the porosity derived from Hg intrusion are provided in Table 2. The change trend of the pore volume was also similar to that of the surface area. Although there were some scatters in the data, the best porosity was achieved by E25 and E31, respectively. Hg intrusion can only detect the pore with

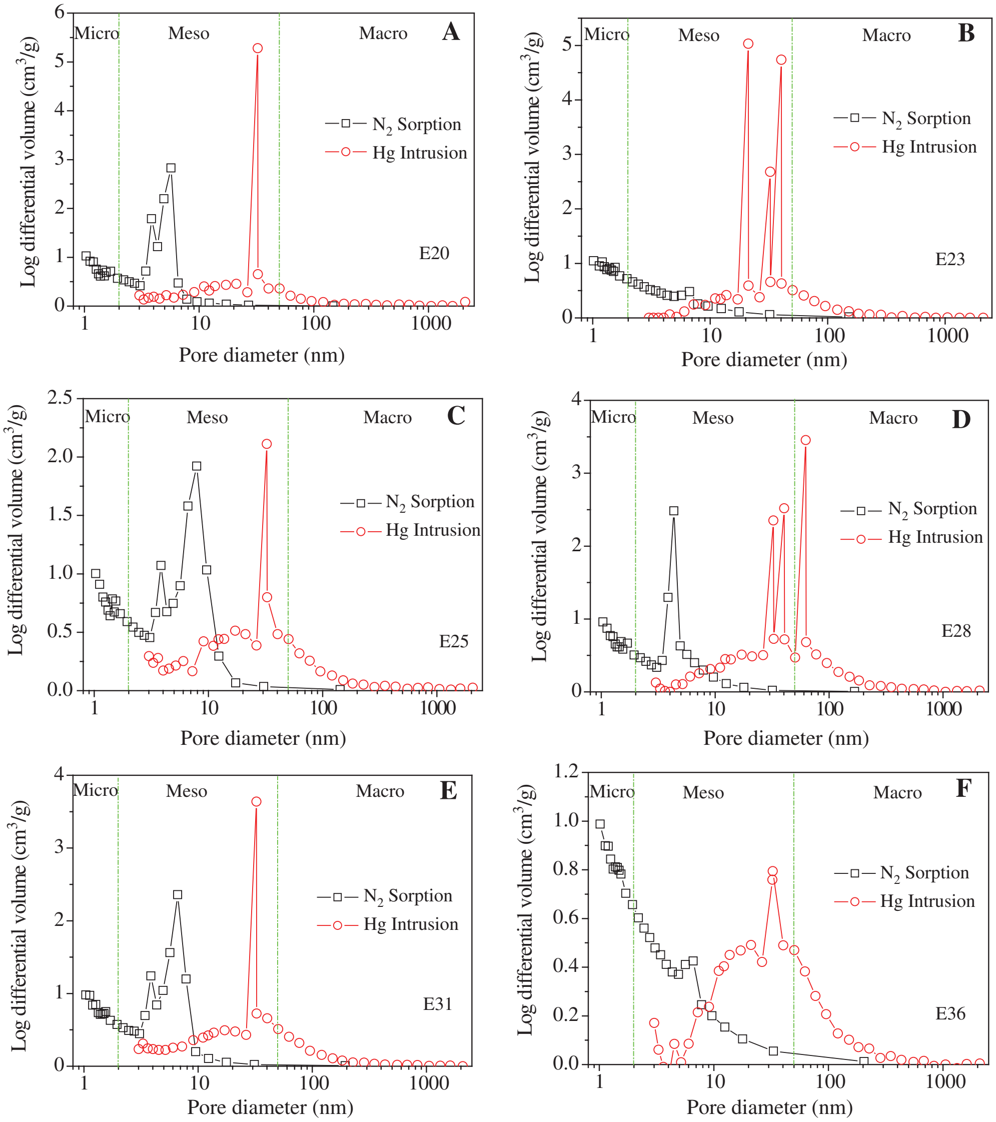

Figure 3: Pore size distribution curves of macroporous PDVB beads prepared with LPE/DCB or HPE/DCB as coporogen. □, curves derived from N_2 sorption; ○, plots originated from Hg intrusion.

diameter no less than 3 nm; therefore, the porosity exhibited different variation trends relative to the pore volume. It could be concluded that excellent pore connectivity will generate high porosity in the mesopore range. Furthermore, the porosity in the macropore range had a rising trend with increasing LPE or HPE level because of much earlier phase separation.

In order to understand more information about micropore (<2 nm), the cumulative pore volume vs. pore diameter is given in Figure 2, which was calculated by Horvath-Kawazoe method (carbon-slit model). As the content of LPE or HPE increased, the curves moved down to that of E20. However, interestingly, the curve of E25 almost overlapped with that of E20, indicative of similar micropore volume. This fact indicated that 5 wt% LPE in coporogen improved both mesoporosity and microporosity of PDVB beads. The latter might be originated from some pore channels between pores. Likewise, the cumulative micropore volume of E31 and E32 was very close to that of E20.

3.3.4 Effects of LPE or HPE on the average pore diameter and size distribution

The pore diameters from N_2 sorption and Hg intrusion are also provided in Table 2. The former technique neglects the largest pores, and the latter ignores the smallest pores.

Therefore, the data derived from the latter were greater than those from the former. Overall, the data from Hg intrusion had a rising trend with increasing LPE or HPE level because of much earlier phase separation.

Pore size distribution curves were calculated from adsorption branch of N_2 sorption and Hg intrusion, and some representative curves are presented in Figure 3. The curve of E20 (Figure 3A) from N_2 sorption exhibited almost all of pores distributed in the micro- and mesopore region, whereas the Hg intrusion-derived curve suggested a large number of mesopores but few macropores.

By contrast, the curve of E23 (Figure 3B) calculated from N_2 sorption showed less mesopore, which explained lower surface area in comparison with E20. However, the mesopore population again increased for E25 (Figure 3C), indicative of good pore connectivity originating from double-phase separation. The curve of E28 (Figure 3D) from Hg intrusion obviously shifted to the macropore range because of much earlier phase separation. The similar trend could be also observed in the curves of PDVB beads prepared with HPE/DCB as coporogen. For example, the curves of E31 (Figure 3E) derived from two methods suggested large numbers of mesopores. After the HPE content amounted to 6 wt% (Figure 3F), the curves revealed obvious features of bimodal pore size distribution, in which one was located in the micropore region and the other situated in the mesopore range.

4 Conclusions

Macroporous PDVB beads were successfully prepared with LPE/DCB or HPE/DCB as the coporogen. Concentration and molecular weight of PE had significant effect on the pore structure of PDVB beads. Combination of high surface area and excellent pore connectivity could be achieved by using 5 wt% LPE or 1 wt% HPE in DCB as coporogen; meanwhile, excellent pore volume was also achieved. In conclusion, PE in combination with DCB provided a novel coporogen to prepare macroporous polystyrene beads with high surface area and pore connectivity. It would be valuable to investigate the mechanism of dependent phase separation, which could be used for fine controlling pore structure of macroporous beads.

Acknowledgment: This work was supported by the National Natural Science Foundation of China under grant no. 51373051.

References

1. Liu QQ, Li YL, Shen SH, Zhou SS. The influence of crosslinking density on the pore morphology of copolymer beads prepared with a novel pore-forming agent. Mater Chem Phys. 2011;125(3):315–8.
2. Tang MY, Huang GB, Zhang S, Liu Y, Li XX, Wang XR, Pang XB, Qiu HX. Low-cost removal of organic pollutants with nickel nanoparticle loaded ordered macroporous hydrogel as high performance catalyst. Mater Chem Phys. 2014;145(3):418–24.
3. Jacukowicz-Sobala J, Drabent K, Kociolek-Balawejder E. Evaluation of ferromagnetic hybrid polymers obtained using cation exchangers. Mater Chem Phys. 2015;161(1):107–15.
4. Liu QQ, Tang Z, Ou BL, Liu LH, Zhou ZH, Shen SH, Duan YX. Design, preparation, and application of ordered porous polymer materials. Mater Chem Phys. 2014;144(3):213–25.
5. Wang ML, Wang CH, Wang W. Synthesis of CdS nanocomposites using macroporous ion-exchange resins. Mater Chem Phys. 2007;104(1):162–5.
6. Bradford EB, Vanderhoff JW. Electron microscopy of monodisperse latexes. J Appl Phys. 1955;26(7):861–71.
7. Ugelstad J, Kaggerud KH, Hansen FK, Berger A. Absorption of low molecular weight compounds in aqueous dispersions of polymer-oligomer particles 2. A two step swelling process of polymer particles giving an enormous increase in absorption capacity. Makromol Chem. 1979;180(3):737–42.
8. Okubo M, Nakagawa T. Preparation of micro-size monodisperese polymer particles having highly crosslinked structures and vinyl groups by seeded polymerization of divinylbenzene using the dynamic swelling method. Colloid Polym Sci. 1992;270(9):853–8.
9. Cheng CM, Micale FJ, Vanderhoff JW, El-Aasser MS. Synthesis and characterization of monodisperse porous polymer particles. J Polym Sci Polym Chem. 1992;30(2):235–44.
10. Cheng CM, Micale FJ, Vanderhoff JW, El-aasser MS. Monodisperse porous polmer particles: formation of the porous structure. J Polym Sci Polym Chem. 1992;30(2):245–56.
11. Wang QC, Svec F, Frechet JMJ. New designs of macroporous polymers and supports: from separation to biocatalysis. Science 1996;273(12):205–11.
12. Galia M, Svec F, Frechet MJ. Monodisperse polymer beads as packing material for high-performance liquid chromatography: effect of divinylbenzene content on the porous and chromatographic properties of poly(styrene-*co*-divinybenzene) beads prepared in presence of linear polystyrene as a porogen. J Polym Sci Polym Chem. 1994;32(11):2169–75.
13. Cheng CM, Micale FJ, Vanderhoff JW, El-Aasser MS. Pore structural studies of mono-disperse porous polymer particles. J Colloid Interf Sci. 1992;150(2):549–58.
14. Wulff G. Molecular imprinting in cross-linked materials with the aid of molecular templates: a way towards artificial antibodies. Angew Chem Int Ed. 1995;34(17):1812–32.
15. Macintyre FS, Sherrington DC. Control of porous morphology in suspension polymerized poly(divinylbenzene) resins using oligomeric porogens. Macromolecules 2004;37(20):7628–36.
16. Liu QQ, Wang L, Xiao AG, Yu HJ, Tan QH, Ding JH. Unexpected behavior of 1-chlorodecane as a novel porogen in the preparation of high-porosity poly(divinylbenzene) microspheres. J Phys Chem C. 2008;112(34):13171–4.
17. Liu QQ, Wang L, Xiao AG, Yu HJ, Ding JH, Tan AH, Hou J. Preparation of poly(divinylbenzene) microspheres with controllable pore

structure using poly(propylene)/toluene as coporogen. J Appl Polym Sci. 2009;113(5):2997–3004.

18. Liang K, Peng MX, Liu QQ. Monodisperse cross-linked polystyrene nanospheres by emulsifier-free miniemulsion polymerization. e-Polymers 2015;15(4):263–70.
19. Xiao AG, Wang L, Liu QQ, Yu HJ, Wang JJ, Hou J, Tan QH, Ding JH, Ding WB, Amin AM. A novel linear–hyperbranched multiblock polyethylene produced from ethylene monomer alone via chain walking and chain shuttling polymerization. Macromolecules 2009;42(6):1834–7.